Growing season CH₄ and N₂O fluxes from a sub-arctic landscape in northern Finland

Kerry J. Dinsmore[1], Julia Drewer[1], Peter E. Levy[1], Charles George[2], Annalea Lohila[3], Mika Aurela[3], Ute M. Skiba[1]

5 [1]Centre for Ecology and Hydrology, Penicuik, EH26 0QB, UK
[2]Centre for Ecology and Hydrology, Wallingford OX10 8BB, UK
[3]Finnish Meteorological Institute, Climate Change Research, FI-00101 Helsinki, Finland

Correspondence to: Kerry J Dinsmore (kjdi@ceh.ac.uk)

Abstract. Subarctic and boreal emissions of CH₄ are important contributors to the atmospheric greenhouse gas (GHG) balance
10 and subsequently the global radiative forcing. Whilst N₂O emissions may be lower, the much greater radiative forcing they
produce justifies their inclusion in GHG studies. In addition to the quantification of flux magnitude, it is essential that we
understand the drivers of emissions to be able to accurately predict climate-driven changes and potential feedback mechanisms.
Hence this study aims to increase our understanding of what drives fluxes of CH₄ and N₂O in a subarctic forest/wetland
landscape, exploring both spatial and temporal variability, and uses satellite derived spectral data to extrapolate from chamber
15 scale fluxes to a 2 x 2 km landscape area.

From static chamber measurements made during summer and autumn campaigns in 2012 in the Sodankylä region of Northern
Finland, we concluded that wetlands represent a significant source of CH₄ (3.35 ± 0.44 mg C m^{-2} hr^{-1} during summer campaign
and 0.62 ± 0.09 mg C m^{-2} hr^{-1} during autumn campaign), whilst the surrounding forests represent a small sink ($-0.06 \pm <0.01$
mg C m^{-2} hr^{-1} during the summer campaign and $-0.03 \pm <0.01$ mg C m^{-2} hr^{-1} during the autumn campaign). N₂O fluxes were
20 near-zero across both ecosystems and as such could not be accurately described as either consistent sinks or sources.

We found a weak negative relationship between CH₄ emissions and water table depth in the wetland, with emissions decreasing
as the water table approached and flooded the soil surface. We attribute this relationship, which initially seems counter to much
of the current literature, to water tables being consistently above the level where a positive relationship would be expected.
Whilst conditions may appear optimal for CH₄ production at higher water tables, reduced diffusivity may reduce the net
25 emissions, indicating a complex interaction of processes which combine to produce the net emission rate measured.
Temperature was also an important driver of CH₄ with emissions increasing to a peak at approximately 12°C. Increases in
temperature beyond 12°C led to a subsequent reduction in emissions, indicating the presence of multiple interacting processes.
A multiple regression modelling approach was used to describe CH₄ emissions based on spectral data from PLEIADES PA1
satellite imagery across a 2 x 2 km landscape. Our best model described 45% of spatial variability using blue and near infra-
30 red bands with the inclusion of the commonly described simple ratio (SR) and normalised difference vegetation index (NDVI).
When applied across the whole image domain we calculated a CH₄ source of 2.05 ± 0.61 mg C m^{-2} hr^{-1}. This was significantly
higher than landscape estimates based on either a simple mean or weighted by forest/wetland proportion (0.99 ± 0.16 mg C m^{-}

^{2} hr^{-1}, 0.93 ± 0.12 mg C m^{-2} hr^{-1}, respectively). Hence we conclude that ignoring the detailed spatial variability in CH$_4$ emissions within a landscape leads to a potentially significant underestimation of landscape scale fluxes.

1 Introduction

Almost a third of the world's soil carbon is estimated to be stored in boreal and sub-arctic wetlands (Gorham, 1991) yet
5   emissions are still poorly constrained (Bridgham et al., 2013). Furthermore, the potential feedbacks between high latitude carbon and the global atmospheric radiative balance is not fully understood or accurately accounted for in coupled carbon cycle-climate models (Koven et al., 2011). It is now accepted that global surface air temperatures are rising and the rate of increase is greatest in these high latitude areas (Pachauri and Reisinger, 2007). Hence understanding both the current magnitude of emissions and the drivers are essential to monitor and predict climate-driven changes and climate feedback mechanisms.
10   Whilst it is important to understand the direct implications of increased temperature on net greenhouse gas (GHG) emissions, it is also critical to consider the indirect impact through secondary drivers such as permafrost thaw, changes in vegetation community structure, substrate availability, soil hydrological regimes and flow path dynamics. These factors, both individually and via interactions, are likely to alter both net GHG emissions and GHG speciation; e.g. a recent meta-analysis showed the temperature sensitivity of CH$_4$ was greater than that of CO$_2$ suggesting increased temperature may lead to changes in the
15   CH$_4$:CO$_2$ emission ratio (Yvon-Durocher et al., 2014). The sensitivity of CH$_4$ fluxes to these environmental controls is not currently well understood, limiting the ability of mechanistic models to accurately simulate actual net fluxes. Hence a significant research focus is required to fully explain the drivers of GHG emissions and therefore provide a solid basis for future prediction.

Overall, boreal forests appear to be a small sink for CH$_4$ and a small source of N$_2$O (Moosavi and Crill, 1997; Pihlatie et al.,
20   2007) whilst wetlands typically represent sources of CH$_4$, and a small sink for N$_2$O (e.g. Bubier et al., 1993; Drewer et al., 2010b; Huttunen et al., 2003). Net CH$_4$ emissions are controlled by the balance of activity between anaerobic methanogenic and oxidizing aerobic methanotrophic bacteria. Hence the degree of soil saturation, which controls the position of the oxic-anoxic boundary and the associated soil redox potential, has been identified as an important driver of net CH$_4$ emission (Bubier et al., 1995; Kettunen et al., 1999; Nykanen et al., 1998). Other factors such as temperature, substrate availability, soil porosity
25   and pH are also commonly reported drivers of CH$_4$ emissions (Baird et al., 2009; Dinsmore et al., 2009b; Levy et al., 2012; Strack et al., 2004; Yvon-Durocher et al., 2014). Whilst the rate of methanogenesis and methanotrophy are both influenced by temperature, methanogenesis is generally considered to be more temperature-sensitive resulting in a positive relationship between temperature and net CH$_4$ emission (Dunfield et al., 1993; van Hulzen et al., 1999). CH$_4$ produced within the soil environment is then transported to the atmosphere via diffusion, ebullition or plant-mediated transport.
30   Vegetation can exert either a direct control on CH$_4$ emission via plant-mediated transport, or indirect control via its contribution to soil structure, moisture, anaerobic microsites and substrate availability. The development of aerenchyma is an adaptation to waterlogged conditions found in many vascular wetland species. Where such species are present they can act as gas conduits,

allowing GHGs produced in the anoxic layer to be transported to the atmosphere with minimal oxidation, subsequently increasing emissions by up to an order of magnitude (Dinsmore et al., 2009a; MacDonald et al., 1998; Minkkinen and Laine, 2006). Vegetation community structure also provides a useful proxy for environmental variables that are themselves difficult to measure, such as long-term water table dynamics (Gray et al., 2013; Levy et al., 2012).

5   The primary processes controlling N_2O emissions from boreal soils are nitrification, where ammonium is oxidised to nitrate under aerobic condition and denitrification, where oxidised nitrogen species are reduced to N_2O or N_2 under anaerobic conditions (Firestone and Davidson, 1989). As N_2O production is again a microbial process and one that is strongly dependent on the ratio of aerobic to anaerobic soil microsites, factors such soil moisture status, temperature, pH, and substrate availability, in particular nitrate and ammonium, are also commonly reported drivers of N_2O emissions (Kettunen et al., 1999). Whereas

10   nitrification is likely to be the dominant process in forests, denitrification is considered the most important source of N_2O in wetlands; further work is still needed before the importance of more recently recognised processes such as anaerobic ammonium oxidation (anammox) can be quantified (Sutton and et al., 2011).

A number of different in-situ methods are available for the measurement of GHG emissions. Eddy covariance methods produce high temporal resolution measurements integrated at the field and ecosystem scale (Baldocchi et al., 2001; Hargreaves and

15   Fowler, 1998); whilst useful for field scale quantification, the method does not allow separation of individual landscape components. Traditional chamber based studies allow a more targeted experimental design where individual microtopographical features or vegetation communities can be selected and compared (Dinsmore et al., 2009b; Drewer et al., 2010a). By explaining small-scale spatial variability we can gain a greater understanding of GHG drivers and begin to predict how climate or land-use management changes will alter the GHG balance over the full landscape.

20   There exists a fundamental mismatch between the scale of measurement required to increase process level understanding of GHG emissions, and the scale required to make useful assertions about the magnitude of emission sources that are relevant to the global GHG budget. Whilst land-surface models provide one way to bridge this mismatch of scale, they are often limited by the availability of specific input variables e.g. water table depth, which cannot be measured at the spatial resolution required to provide an accurate output. As a result, modelled estimates of northern high-latitude wetland CH_4 sources are highly variable

25   between studies ranging from approximately 20 - 157 Tg CH_4 yr^{-1} (Zhu et al., 2013 and references therein). An alternative method of upscaling is empirically mapping emission factors onto spectral data provided by high resolution satellite imagery. This method utilises the spectral signatures of different vegetation types and vegetation specific differences in GHG emissions to create a landscape scale emission map.

In this study we use static-chambers and satellite imagery to assess the primary spatio-temporal drivers of GHG emissions in

30   sub-arctic/boreal Finland and upscale this to a 4 km^2 landscape containing both forest and wetland ecosystems.

2 Methods

2.1 Site Description

The Arctic Research Centre of Sodankylä (67°22'N 26°39'E, 179 m a.s.l.) is located in central Lapland, Northern Finland, approximately 100 km north of the Arctic Circle. The centre is run by the Finnish Meteorological Institute, is part of the

5 Pallas-Sodankylä GAW station and includes a level 1 ICOS ecosystem station. Whilst referenced as an Arctic site in respect to stratospheric meteorology and geographical location, it is considered to be within the sub-arctic/boreal vegetation zone. Mean annual temperature and precipitation on site from 1981-2010 was -0.4°C and 527 mm, respectively. Records of mean annual air temperature on site have shown an increase of 0.02°C yr^{-1} over the period 1961-2000; the rate of increase specifically during March to May was 0.04°C yr^{-1} (Aurela et al., 2004; Tuomenvirta et al., 2001).The mean snow depth (mid-March) is 75

10 cm with median snow cover start and end dates of 26th September and 14th May (Finnish Meteorological Institute). Scots pine forests and wetlands are the two dominant ecosystems in this region. Both ecosystems were covered by the greenhouse gas flux measurements in order to enable the landscape scale upscaling of the results.

The forest (N67°21.708' E26°38.290', 179 m.a.s.l.) is classified as an Uliginosum-Vaccinium-Empetrum (UVET) type Scots pine (*Pinus sylvestris*) forest on a sandy podzol. The mean vegetation height within the forest is 12 m in the area our

15 measurements were made with an average stand age of 60-100 years and tree density of 2100 ha^{-1}. The forest floor contains a varying degree of lichen (*Cladonia* spp.) which is heavily dependent on the presence/absence of reindeer. We located static chambers evenly between 3 forest sites (unfenced, 15 year enclosure, 50 year enclosure) to ensure variability in GHG emissions due to lichen cover was included in our results. The nearby Halssiaapa wetland (N67°22.111' E26°39.269', 180 m.a.s.l.) is a eutrophic flark fen dominated by large, treeless flarks with abundant sedge vegetation and intermittent brown moss and

20 *Sphagnum* cover. Intermediate, low ridges consist of birch fen vegetation interspersed with pubescent birch trees (*Betula pubescens*), with a dominant height of approximately 5-7 m. The most common shrubs are *Betula nana*, *Andromeda polifolia* and *Vaccinium oxycoccos*, herbaceous plants are primarily *Potentilla palustris* and *Menyanthes trifoliata*, and grasses are predominantly *Care*x species (several different species observed) or *Scheuchzeria palustris*. When set within a wider 2 x 2 km landscape unit (to which we will upscale measurements), the proportion of wetland to forest was almost 2:1 with wetlands

25 making up 61% of the area, and forests 32%. The remaining 7% included open water and grass, bare soil and buildings primarily associated with the Sodankylä Arctic Research Centre. Within the larger regional area described in an associated study by O'Shea et al. (2014) (http://www.eea.europa.eu/data-and-maps/data/corine-land-cover-2006-raster) forests made up a much greater proportion of the landscape with coniferous and mixed forests representing 33% and 16% of the land area, respectively, and wetlands 23%.

2.2 Field Methodology

Measurements were carried out during growing season 2012 in two measurement campaigns (Summer: 12th July – 2nd August; Autumn: 22nd September – 14th October), with the intention of capturing peak summer CH_4 emissions and the subsequent shoulder season.

5 A total of 60 static chambers were measured, 21 within the forest and 39 within the wetland. Within the forest, 7 chambers were located in each of three subplots representing no enclosure, 12 year enclosure (built in summer 2000) and an approximately 50 year enclosure. Within the wetland, chambers were strategically located to cover the perceived range of both vegetation communities and water table depths. Fluxes were measured on approximately 2 day intervals resulting in a total of 10 measurements for all chambers during the summer campaign, and 7 for the forest and 8 for the wetland chambers
10 during the autumn campaign.

Static chambers were constructed from 40 cm diameter opaque polypropylene pipe following the guidelines discussed in Clough et al. (2015). Shallow bases (10 cm depth) were inserted into the ground the day before the first sampling; bases were left in-situ for the remainder of the study period. Fluxes calculated from the first sampling day were not significantly different from subsequent sampling occasions, the short settling period after base installation is therefore considered to have had no
15 significant effect on subsequent fluxes, and therefore were included in the data analysis. Chamber lids, consisting of a 25 cm section of polypropylene pipe with a closed metal top and pressure compensation plug, were attached and sealed to the in-situ bases during the 45 min flux measurement period. Chamber air (100 ml) was sampled 4 times throughout the approximately 45 minute sampling period and flushed through 20 mL glass vials sealed with butyl rubber plugs. Vials were returned to the laboratory at the Centre for Ecology and Hydrology, Edinburgh, for analysis within approximately one month. Samples were
20 analysed on an HP5890 Series II gas chromatograph (Hewlett Packard (Agilent Technologies) UK Ltd, Stockport, UK) with electron capture detector (ECD) and flame ionisation detector (FID) for N_2O (detection limit<7 µg l−1) and CH_4 analysis (detection limit<70 µg l−1), respectively. Soil temperature was recorded at a depth of 10 cm from four replicate points immediately outside the chamber bases on each sampling occasion using the Omega HH370 temperature probe (Omega Engineering UK Ltd.,Manchester, UK). Within the forest plots, 4 replicate volumetric soil moisture content (VMC)
25 measurements were made, adjacent to each chamber base, using a Theta probe HH 2 moisture meter (Delta T-Devices, Cambridge, UK). Within the wetland, a total of 21 dip wells constructed from 5mm internal diameter pipe, were installed either adjacent to, or where chambers were located close together, between chamber bases. All wetland chambers had at least 1 dip well located within a 50 cm radius, where more than one dip well was located equidistant from the chamber, the mean water table depth from the adjacent dip wells was calculated. Soil respiration (including respiration from the ground
30 vegetation), was measured using a PP-Systems SCR-1 respiration chamber (10 cm diameter) attached to an EGM-4 infrared gas analyser (IRGA,PP Systems; Hitchin, Hertfordshire, England) on each sampling occasion. Soil respiration was measured adjacent to each forest chamber and adjacent to 14 chambers within the wetland, chosen to cover the perceived range of spatial variability. Vegetation within each chamber was recorded upon visual inspection.

A pair of cation and anion Plant Root Simulator (PRS)^{TM} probes were deployed adjacent to each of the 60 chamber bases during both sampling campaigns. During the summer campaign probes were deployed on the 11th and 12th July, and recovered on the 1st August. During the autumn campaign forest probes were deployed on the 22nd and 23rd September and recovered between the 13th and 15th October. As part of the standard analytical processing, concentrations from each probe are corrected

5 for length of deployment. After recovery, probes were processed and cleaned with deionised water following the standard procedure supplied by the manufacturers and returned to Western Ag Innovations Inc., Canada for analysis.

2.3 Data Analysis

Fluxes from static chambers were calculated using GCFlux, version 2, which calculates fluxes based on 5 methods before choosing the most appropriate fit for individual chamber sets (Levy et al., 2011). Reported CH_4 fluxes correlate to the best-fit

10 model for individual chambers (either linear or asymptotic). Due to the larger uncertainty in calculated N_2O concentrations which are often close to the GC detection limits, reported N_2O fluxes were calculated from the linear model approach only. Instantaneous fluxes are presented in units of nmol m^{-2} s^{-1}.

The data distribution of fluxes, from all chambers, and over the full study period, had a strong positive skew (Figure 1). To summarise the data and account for the skewed distributions, geometric means were calculated across time points for all

15 chambers. Where periods of uptake and emission were both present within a time series, geometric means were calculated for each flux direction independently. The presented geometric means are the frequency-weighted sum of emissions and uptake. Upscaled emission estimates are presented in units of either g C m^{-2} hr^{-1} or g N m^{-2} hr^{-1} for CH_4 and N_2O, respectively.

To summarise the complex vegetation and soil data, principal component analyses (PCA) were performed using the princomp function within the R stats package (R version 3.1.1), this uses a spectral decomposition approach which examines the

20 covariances and correlations between variables. Correlation analyses were carried out with principal components one, two and three (PC1, PC2, PC3) against CH_4 fluxes and the most appropriate component taken forward into subsequent explanatory models. No attempt to correlate vegetation or soil components was made with N_2O fluxes given the high uncertainty in the near-zero fluxes.

Spatial variability between chambers on all sampling occasions was large. To allow temporal variability to be considered it

25 was necessary to group chambers. Rather than subjectively assign chambers to groups based on observed landscape features we carried out a cluster analysis (R, version 3.1.1) based on emission rates. This method produced independent groups which could also be used in further analyses to consider the environmental controls of emissions. The total number of clusters was chosen to be 5, after multiple cluster analysis runs this was considered the most appropriate number taking into consideration the complexity for further analyses and clear distinctions between groups.

30 Optical remote sensing imagery was acquired by the Pleiades satellite on 28th August 2012. This provided data in the blue, green, red, and near-infrared (NIR) part of the spectrum for the 2 x 2 km region around the chamber sites, with 2 m resolution on the ground. From these data both the simple ratio (SR = NIR / Red) and normalised difference vegetation index (NDVI = [NIR - Red] / [NIR + Red]) were calculated. The optical data for each chamber location were extracted and related to the

geometric mean of the CH_4 flux at that location. Multiple regression modelling was then carried out using R (version 3.1.1) to describe the CH_4 fluxes of individual chambers initially utilising all four wavebands and the two calculated ratios. The best fit model was used to upscale CH_4 fluxes to the full image domain (4 km^2). Due to large uncertainties in the flux estimates and subsequent inability to accurately model the data, upscaling of N_2O emissions was not carried out using satellite imagery.

5 **3 Results**

Confidence intervals calculated from each chamber measurement, which include errors introduced by a combination of natural variability in the flux over the measurement period, methodological and analytical limitations and uncertainty in model fitting, show a high proportion of calculated fluxes which are indistinguishable from zero. Given the high variability and low fluxes in N_2O, only 8 and 9 % of fluxes were significant in the wetland and forest, respectively. For CH_4, whilst only 56% of fluxes

10 were significantly different from zero in the forest, the wetland was much clearer with zero excluded from the confidence range in 94% of cases.

When separated by site (forest, wetland) and by campaign period (summer, autumn) the highest instantaneous CH_4 fluxes, greatest skew and largest range were all observed in the wetland chambers during the summer period (Figure 1). These equated to a mean flux of 3.35 ± 0.44 mg C m^{-2} hr^{-1}, compared to only 0.62 ± 0.09 mg C m^{-2} hr^{-1} in the wetland during the autumn

15 period. The mean CH_4 flux across the whole measurement period represented an emission of 1.56 ± 0.20 mg C m^{-2} hr^{-1} from the wetland chambers, compared to a mean uptake of 0.04 ± <0.1 mg C m^{-2} hr^{-1} from the forest chambers (Table 1).

N_2O fluxes had a mean emission across the full sampling period of 1.06 ± 0.44 µg N m^{-2} s^{-1} and 0.73 ± 0.40 µg N m^{-2} s^{-1} from forest and wetland chambers, respectively (Table 1).

3.1 Spatial Variability

20 Surface cover data (vegetation and presence of standing water) was summarised using a PCA analysis; combined the top three principal components explained 51% of the total variation between chamber vegetation communities, with principal components 1, 2 and 3 (PC1, PC2, PC3) explaining 24%, 15% and 11%, respectively. PC1, PC2 and PC3 were subsequently tested for correlations with CH_4 fluxes. Spatial variability in CH_4 emissions among wetland chambers was best captured using PC2 (r = 0.40, P <0.01). PC2 also correlated strongest with CH_4 emissions when all chambers (both wetland and forest) were

25 included (r = 0.31, P < 0.01), however PC1 showed the best correlation with forest chambers alone (r = 0.25, P <0.01). PC2 was therefore used throughout future analysis to describe the spatial variability in CH_4 emissions.

PC2 (which best described CH_4 fluxes) showed a strong dependence on the proportion of green *Sphagnum* species within the chamber with positive PC2 values indicating a high prevalence (Figure 2). Due to the strongly non-normal distribution of the data, *Sphagnum* sp. alone could not be correlated with emissions thus the principal component method provides an indirect

30 measure of the relationship. Low PC2 scores indicate a higher abundance of non-*Sphagnum* moss species and high proportion of open water within the chambers. Of the measured environmental variables relating to spatial variability (soil temperature,

soil moisture, water table depth and soil respiration), PC2 only correlated significantly with water table depth (r = 0.17, P < 0.01) with PC2 scores increasing with water table depth.

A similar PCA analysis was carried out to summarise the available soil concentration data. The first three principal components combined explained 56% of total variation with PC1, PC2 and PC3 individually accounting for 31%, 15% and 10% of

5   variability, respectively. PC1 gave the best correlation with CH_4 emissions when all data was combined and for forest chambers alone. PC2 gave a better correlation with wetland chambers alone (PC2: r = 0.40, P < 0.01). PC2 was therefore utilised throughout the remainder of the analysis due to the greater magnitude of wetland versus forest CH_4 emissions, and their subsequent importance to landscape scale emissions.

PC2 was influenced strongly by total N and NH_4^+ concentrations with high concentrations resulting in a low PC2 score (Figure

10   3). The only environmental variable significantly correlated with PC2 was water table depth (r = 0.19, P < 0.01) with high PC2 scores indicating a deep water table. However, when wetland chambers were considered alone soil respiration also showed a significant positive correlation with PC2 (r = 0.31, P < 0.01).

Spatial variability in GHG emissions were tested against the measured environmental variables as well as the most appropriate PCA score for both vegetation and soil, as described above. CH_4 flux was not statistically correlated to water table depth in the

15   wetland chambers (Figure 4). However a relatively strong positive correlation was seen between CH_4 flux and the PCA score from the vegetation analysis; a high score from the vegetation principal component represented a deep mean water table depth. Positive correlations were also found between CH_4 flux, mean soil temperature and the principal component from the soil analysis when the wetland chambers were considered alone. Within the forest chambers, only the soil principal component was statistically correlated CH_4 flux.

20   To further summarise the CH_4 data and provide a method for both upscaling and consideration of temporal variability, chambers were grouped independently based on net emissions. Data distributions within each cluster group are shown in Fig. 5. The cluster identified with the lowest emissions contained all the forest chambers and an additional two low emitting wetland chambers; for explanatory purposes this cluster is subsequently referred to as the 'forest' cluster. The remaining clusters, with sequentially increasing emissions, are labelled wetland_a, wetland_b, wetland_c and wetland_d, respectively.

25   ANOVA showed significant between cluster variability in all tested environmental variables (soil temperature, water table depth, soil respiration, vegetation principal component and soil principal component) with the exception of water table depth (Figure 6). The patterns in soil temperature, PCA_veg and PCA_soil are in line with the previously discussed correlation analysis. When the components of PCA_veg are considered independently the results highlight the importance of *Sphagnum* cover and open water in controlling the CH_4 emissions within the wetland clusters, however this relationship is complicated

30   by the high variability shown by large standard deviations from the mean cluster values (Table 2). Wetland clusters 'a' and 'b', which represent the two lowest emitting wetland groups, had the lowest proportions of *Sphagnum* moss species and the greatest proportion of chambers containing open water.

Between-group differences in soil nutrient concentrations were also considered using ANOVA; only nutrients which displayed significant between group differences are displayed in Fig. 7. The strongest between group difference was evident in the soil

Fe concentrations, with high Fe linked to high CH_4 emitting chambers (F = 62.0, P < 0.01); positive correlations with mean group CH_4 emissions were also seen for B (F = 49.2, P < 0.01), Zn (F = 39.0, P < 0.01) and Mg (F = 49.2, P < 0.01). Negative correlations were seen between mean group CH_4 emission and K (F = 10.6, P < 0.01), NO_3-N (F = 6.38, P < 0.01), and NH_4-N (F = 6.36, P < 0.01). Within the wetland, total-N was lowest in groups with the highest CH_4 emission; however the pattern

5 is less clear when forest chambers are included as these displayed a wide range of total-N but a low CH_4. Only the forest had distinct soil Ca concentrations.

3.2 Temporal Variability

Temporal variability, summarised by cluster, is displayed in Fig. 8 for both the summer and autumn campaign periods. CH_4 emissions remain relatively constant throughout both campaign periods despite a significant drop in emissions between them.

10 Despite the low temporal variability, emissions appear to peak around mid-July in the higher emitting chamber clusters (e.g. wetland_c and wetland_d).

CH_4 emissions did not follow linear relationships with the measured environmental variables (soil temperature, air temperature, water table depth and soil respiration) (Figure 9). CH_4 emissions peaked at a soil temperature of approximately 12°C and an air temperature of approximately 15°C, after which they began to fall. The time series suggests a general decrease in CH_4

15 emissions with rising water table, however the relationship appears to be chamber specific and non-linear suggesting a greater complexity than is usually accounted for. In the high emitting chambers, there is a peak in CH_4 emissions as the water level reaches the surface, the emissions drop until water tables of approximately 5 cm depth and then rise again as the water level deepens further. Chamber clusters associated with lower total CH_4 emissions did not show this peak associated with surface water tables but instead followed a smoother, but still non-linear, increase in emissions with increasing water table depth. No

20 relationship was observed between soil temperature and water table depth ruling out a potential interaction as the cause of the peaks associated with particular water table depths or soil temperatures.

3.3 Spectral analysis and upscaling

A multiple regression model including blue, green, red, NIR, SR and NDVI explained 45 % of the variance in the spatial methane flux. Transformations of the data and more complex models were explored, but did not substantially improve the

25 model fit. A simpler model containing only SR, NDVI and the blue and NIR wavebands performed equally as well as the full model also explaining 45% of the spatial variation (Table 3), this simpler model was therefore used in subsequent analysis. To predict mean methane flux at landscape scale, we applied the regression model to the optical data over the whole 2 x 2 km domain. This predicted high methane fluxes in the wetland areas in the north-east and at forest edges (Figure 10). Using the optical data to scale up the chamber measurements, the mean methane flux over the whole domain is estimated to be 47.4 ±

30 14.1 nmol CH_4 m^{-2} s^{-1} or 2.05 ± 0.61 mg C m^{-2} hr^{-1}. By comparison, if the flux over the whole spatial domain were estimated simply as the arithmetic mean of the individual chamber measurements (geometric mean to summarise temporal variability) the value would be significantly lower (23.0 ± 3.78 nmol CH_4 m^{-2} s^{-1}). If we account for the differences between wetland and

forest alone using an appropriate area weighting factor, ignoring variability within these landscape units, estimated emissions are 21.6 ± 2.85 nmol CH_4 m^{-2} s^{-1}, also substantially lower than our modelled approach.

4 Discussion

Fluxes of CH_4 from the forest and wetland areas within the landscape were significantly different at $-0.06 + <0.01$ and $3.35 \pm$
5   0.44 mg C m^{-2} hr^{-1}, respectively. Whilst the error displayed here suggests confidence in the forest as a net sink for CH_4, when individual chamber measurements are considered, only 56.3% of the measured fluxes had an error bar that did not cross the zero line. Hence we can only be confident that the sign of the flux is correct in just over half of our forest data. On removal of all fluxes with an uncertain sign, the mean remains negative in the forest chambers. This gives confidence that whilst the calculated flux is very small, it is a small sink rather than a source. In the wetland however, 94.4% of the measured fluxes
10 differed significantly from zero, so we can be confident that the wetland represented a strong source of CH_4.
A similar analysis was carried out on the N_2O flux data and here due to very high uncertainties in the sign of individual flux measurements (only 8.68% and 7.79% of measurements in the forest and wetland, respectively, did not have error bars crossing the zero line) we cannot differentiate either the forest or wetland as being a net sink or source over the campaign period. We can simply state that N_2O fluxes in both landscape units were near-zero. Due to consistently near-zero fluxes, little could be
15 concluded about the drivers of N_2O emissions over within our landscape area.

4.1 Drivers of CH_4 emissions

The relationship between CH_4 emissions and water table position was not straightforward. Considering the mean CH_4 flux for each chamber and testing this against the mean water level position of that chamber showed no significant relationship (Figure 4), suggesting water table was not an important factor in controlling spatial variability in emissions across the site. Furthermore,
20 when chambers were clustered based on their CH_4 emissions, there was high within-group variability in water table and subsequently no significant differences in water table between groups (Figure 6). Whilst much of the previous literature suggests water level as the primary driver of CH_4 (Aerts and Ludwig, 1997; Hargreaves and Fowler, 1998; Waddington et al., 1996) due to its role in controlling the oxic/anoxic boundary, there is a growing body of evidence which suggests this is true only in drier ecosystems (Hartley et al., 2015; Olefeldt et al., 2013; Turetsky et al., 2014. The water levels used in this analysis
25 only represented the water level during the campaign periods, with no consideration of longer term means. Due to the presence of alternative electron acceptors and the delay in returning to favourable redox conditions, fluctuations in the water level can result in a reduced population and a subsequent reduction in CH_4 production, even after water levels and anoxic conditions recover (Freeman et al., 1994; Kettunen et al., 1999). Hence whilst soil conditions may appear suitable for CH_4 production at the time of measurement, an unfavourable water table in the days to weeks prior to the measurement can limit methanogenesis
30 and mask the expected relationship.

CH_4 in the wetland correlated positively and significantly with a component from the vegetation PCA analysis. The vegetation component that best described CH_4 emissions (PC2) related primarily to *Sphagnum* cover within the chambers and also linked low scores to a high proportion of open water. *Sphagnum* is an indicator of long term near-surface water table position, hence whilst the directly measured water table did not correlate significantly with CH_4 emissions, the vegetation analysis suggests

5   that longer term water level conditions do correlate with spatial variability in CH_4.

The relationship is further complicated by the presence of standing water which related to low emitting chambers. This may be a consequence of reduced diffusion from the soil to the atmosphere rather than a result of reduced production. If standing water remains for long periods of time, the sustained anoxic conditions can alter the vegetation and soil chemistry. For example reduced nitrification, an oxic process, can lead to a build-up of NH_4^+ in water logged conditions. Soil PCA component 2 which

10   correlated positively with CH_4 emissions showed a strong link to the concentration of NH_4^+; high concentrations were linked to low PCA scores and low CH_4 emissions. NH_4^+ in this case may be acting as an indicator of the chambers which were inundated with surface water for sustained time periods.

Our chambers were not specifically designed to measure emissions from water surfaces and as a result cut out all wind driven turbulence which is likely to be an important driver of the evasion flux (MacIntyre et al., 1995). It is therefore difficult to

15   identify whether standing water produced a decrease in CH_4 production, a real decrease in flux due to low diffusivity through the water column, or if our results were a consequence of our methodology artificially reducing gas transfer across the water-air boundary. A previous study showed an increase in CH_4 emissions along a water table gradient from 35 cm depth to 5 cm above the soil surface. Above 5 cm the relationship with increasing water level was negative (Pelletier et al., 2007). Whilst our results are not as clear as those presented by Pelletier *et al.* (2007) a similar mechanism of reduced CH_4 diffusion through

20   standing water may be responsible in both cases.

Figure 7 shows a clear positive relationship between Fe, Zn and CH_4 emissions, with high emitting clusters also displaying the highest concentrations. These cations reflect the redox potential of the soil with increasing concentrations indicating a lowering of the redox potential. The CH_4 water table relationship is indirect with water table used as a proxy for soil oxygen content and redox potential. Here we find cation concentrations have a greater explanatory power than water table hence they may

25   represent a more appropriate indicator of soil redox status and methanogenic potential.

When we consider the temporal patterns in CH_4 emissions across the 2 campaign periods we see a similar response as in the spatial analysis, with emissions falling as the water level rises between approximately 15 and 5 cm depth. No relationship was found between water table and soil temperature ruling out an interaction as the primary cause of the water table relationship. Tupek *et al.* (2014) measured increasing CH_4 emissions in response to a rising water table until a peak at approximately 20 cm

30   depth in a central Finnish mire, after which the relationship changed with emissions decreasing as the water table approached the surface. Water table depths measured in this study covered a smaller range and therefore we can assume similar dynamics may be apparent if the water level was to drop below 20 cm. Similarly a recent synthesis (Turetsky et al., 2014) involving 71 wetlands found the optimum water table depth for CH_4 emissions to be 23.6 ± 2.4 cm for bog ecosystems. Again suggesting the negative water table relationship observed here is due to water table depth being consistently above the optimum. As the

water table rose between 5 cm depth and the soil surface, emissions appear to increase again peaking at approximately the soil surface and then decreasing with increasing water depth above the soil surface. This could be due to physical forcing of CH_4 out of the soil pore space as it reaches the soil surface. Importantly, what our results clearly show are that there are a number of driver mechanisms interacting to produce the observed CH_4-water table relationship.

5   A significant positive spatial relationship was seen between soil temperature and CH_4 (Figure 4 and Figure 6). The relationship between CH_4 emission and temperature is a well-established one often observed in the literature (Segers, 1998) as a result of the greater sensitivity of methanogenesis than methanotrophy; however most studies focus on the implications of temporal variation rather than the spatial pattern. The spatial variability in soil temperature is likely to be linked to a combination of soil water content and the surface reflectance of the vegetation cover. Changing soil temperature therefore represents an important

10   by-product of other environmental changes that needs to be accounted for in predictive mechanistic models.

The temporal relationship between CH_4 emissions and temperature showed a Gaussian response curve typical of microbial control. Peak CH_4 emission occurred at a soil temperature of ~12°C. A similar pattern was observed in a central Finland mire by Tupek *et al.* (2014) who recorded a peak in emissions corresponding to 14°C.

4.2 Upscaling

15   The wetland CH_4 fluxes calculated here (3.35 mg C m^{-2} hr^{-1} during the summer season and 1.56 mg C m^{-2} hr^{-1} when the autumn period is included) are similar in magnitude to those described in a multisite analysis by Turesky et al. *(2014)* for subarctic (3.51 ± 0.19 mg C m^{-2} hr^{-1}) and boreal wetlands (2.27 ± 0.04 mg C m^{-2} hr^{-1}). However given the large differences between fluxes calculated within the forest and wetland, and the heterogeneous mix of these two primary ecosystem types across the subarctic/boreal system, landscape scale emissions are of greater importance in understanding global CH_4 source estimates

20   than wetland emissions alone. By extending our sampling site to a 2 x 2 km landscape we can calculate emissions which are more relevant to the region as a whole. Based on a weighted average of fluxes from the forest and wetland within the landscape, and assuming CH_4 emissions from the other landscape units are zero, we can calculate average landscape scale emissions of 0.93 ± 0.12 mg CH_4-C m^{-2} hr^{-1}.

However, whilst calculations at this level of detail have previously been shown to give good agreement with more

25   top down methodologies (O'Shea et al., 2014), significant information is lost regarding spatial variability which we have already shown to be large, especially within the wetland. Utilising spectral data across the 2 x 2 km landscape and a multiple regression model, we calculated average CH_4 flux over the growing season as 47.4 ± 14.1 nmol CH_4 m^{-2} s^{-1} or 2.05 ± 0.61 mg C m^{-2} hr^{-1}. This is significantly higher than the landscape scale CH_4 flux of 1.1 to 1.4 g CH_4 m^{-2} during the May to October growing season (0.19 to 0.23 mg C m^{-2} hr^{-1}) calculated by Hartley et. al. (2015) from field measurements collected

30   approximately 240 km north of our study site, up-scaled using aerial imagery and satellite data. Even when utilising data presented from only July-September, Hartley et al. (2015) still recorded much lower landscape scales fluxes (approx.. 0.24 mg C m^{-2} hr^{-1}) than this study due to the different landscape units and proportions of vegetation communities.

There is still considerable uncertainty in extrapolating to our 2 x 2 km landscape despite optical remote sensing data having complete coverage and a reasonably well-defined relationship with CH$_4$ flux. Greatest emissions and subsequently the greatest uncertainty are observed in an area to the north east of our landscape which represents an area of yellow/green *Sphagnum*. Whilst useful as an upscaling tool over this small landscape area, this method relies on local chamber measurements and is therefore not appropriate for extrapolation to larger spectral datasets. Equally, as demonstrated in the comparison with Hartley et al. (2015), who's study landscape is in relatively close proximity to that considered here, the variability in ecosystem features across the region is extremely important, therefore larger regional scale estimates cannot be achieved by extrapolating from the land-scape mean presented here without significant further research effort.

4.3 Conclusions

Our results showed a significant proportion of measured N$_2$O fluxes, across both wetland and forest, and CH$_4$ fluxes within the forest, were not distinguishable from zero. Considering only those fluxes that did differ significantly from zero we can be confident that the wetland represented a strong source of CH$_4$, especially during the summer peak growing season (3.35 ± 0.44 mg C m^{-2} hr^{-1}), and the forest a small CH$_4$ sink (summer: -0.06 ± <0.01 mg C m^{-2} hr^{-1}). We can only conclude that N$_2$O fluxes were near-zero across the landscape.

We did not observe a direct water table control on spatial variability in CH$_4$ emissions but instead found a relationship with vegetation communities, in particular the presence of *Sphagnum* mosses, and with soil chemistry which we attribute to redox potential. Both these parameters suggest that water table level and water table variability over a longer time scale prior to flux measurements is required to accurately predict CH$_4$ emissions. When temporal variability across the campaigns was considered we found a decrease in CH$_4$ emissions as water table approached the soil surface and the soil became fully saturated. We attribute this apparent reversal of the literature described relationship between CH$_4$ and water table to the water table depth being consistently above the optimum. As water levels continue to rise beyond this point diffusion becomes restricted and the flux diminished. We also found a temporal relationship between CH$_4$ emissions and temperature with peak emissions at approximately 12°C.

To upscale the chamber measurements of CH$_4$ to a 2 x 2 km landscape area we utilised PLEIADES PA1 satellite imagery and could account for 45% of spatial variability in CH$_4$ flux using SR, NDVI, Blue and NIR spectral data. Applying this model to the full area gave us an estimated CH$_4$ emission of 2.05 ± 0.61 mg C m^{-2} hr^{-1}. This was higher than landscape estimates based on either a simple mean or weighted by forest/wetland proportion alone (0.99 ± 0.16 mg C m^{-2} hr^{-1}, 0.93 ± 0.12 mg C m^{-2} hr^{-1}, respectively). Hence whilst there are clearly uncertainties associated with the modelled approach, excluding spatial variability as with the latter two methods is likely to lead to underestimations in total emissions. Whilst the modelled extrapolation method described here is unlikely to be accurate over a large regional area, we conclude that over an area similar in size to our 2 x 2 km landscape, it is a useful upscaling tool.

Data availability

Data will be made available through the Environmental Information Data Centre (EIDC), a Natural Environment Research Council data centre hosted by the Centre for Ecology & Hydrology (CEH), UK.

Author contribution

5   J. Drewer, U.M. Skiba and K.J. Dinsmore designed and carried out the field experiments and subsequent laboratory analysis. A. Lohila and M. Aurela provided help with the experimental set-up, selection of the field site and local knowledge. P.E. Levy and C. George analyzed the spectral data and developed the model for upscaling chamber emissions to landscape. K.J. Dinsmore carried out the remainder of the analysis and prepared the manuscript with contributions from all co-authors.

Acknowledgements

10   This work was funded through the MAMM project (Methane and other greenhouse gases in the Arctic: Measurements, process studies and Modelling, http://arp.arctic.ac.uk/projects/) by the UK Natural Environment Research Council (grant NE/I029293/1).

We wish to thank staff from the Finnish Meteorology Institute at Sodankylä and Helsinki, in particular Annalea Lohila, Tuula Aalto and Tuomas Laurila for their kind hospitality, invitation and collaboration and the EU project InGOS for supporting the

15   two field campaigns in Sodankylä through the TNA2 travel budget (*www.**ingos**-infrastructure.eu/access/**tna2**-access-to-stations).*

References

Aerts, R. and Ludwig, F.: Water-table changes and nutritional status affect trace gas emissions from laboratory columns of peatland soils, Soil Biology & Biochemistry, 29, 1691-1698, 1997.

20   Aurela, M., Laurila, T., and Tuovinen, J.-P.: The timing of snow melt controls the annual CO_2 balance in a subarctic fen, Geophysical Research Letters, 31, L16119, 2004.

Baird, A. J., Belyea, L. R., and Morris, P. J.: Upscaling of peatland-atmosphere fluxes of methane: Small-scale heterogeneity in process rates and the pitfalls of bucket-and-slab models. In: Carbon Cycling in Northern Peatlands, Geophys. Monogr. Ser., AGU, Washington, DC, 2009.

25   Baldocchi, D., Falge, E., Gu, L. H., Olson, R., Hollinger, D., Running, S., Anthoni, P., Bernhofer, C., Davis, K., Evans, R., Fuentes, J., Goldstein, A., Katul, G., Law, B., Lee, X. H., Malhi, Y., Meyers, T., Munger, W., Oechel, W., U, K. T. P., Pilegaard, K., Schmid, H. P., Valentini, R., Verma, S., Vesala, T., Wilson, K., and Wofsy, S.: FLUXNET: A new tool to study

the temporal and spatial variability of ecosystem-scale carbon dioxide, water vapor, and energy flux densities, Bulletin of the American Meteorological Society, 82, 2415-2434, 2001.

Bridgham, S. D., Cadillo-Quiroz, H., Keller, J. K., and Zhuang, Q.: Methane emissions from wetlands: biogeochemical, microbial, and modeling perspectives from local to global scales, Global Change Biology, 19, 1325-1346, 2013.

5 Bubier, J., Moore, T. R., and Juggins, S.: Predicting methane emission from bryophyte distribution in northern peatlands, Ecology, 76, 677-693, 1995.

Bubier, J. L., Moore, T. R., and Roulet, N. T.: Methane emissions from wetlands in the midboreal region of northern Ontario, Canada. Ecology. 1993. 74, 1993.

Clough, T. J., Rochette, P., Thomas, S. M., Pihlatie, M., Christiansen, J. R., and Thorman, R. E.: Chamber Design. In: Nitrous
10 Oxide Chamber Methodology Guidelines, de Klein, C. A. M. and Harvey, M. J. (Eds.), 2, Ministry for Primary Industries, Wellington, New Zealand, 2015.

Dinsmore, K. J., Skiba, U. M., Billett, M. F., and Rees, R. M.: Effect of water table on greenhouse gas emissions from peatland mesocosms, Plant and Soil, 318, 229-242, 2009a.

Dinsmore, K. J., Skiba, U. M., Billett, M. F., Rees, R. M., and Drewer, J.: Spatial and temporal variability in CH_4 and N_2O
15 fluxes from a Scottish ombrotrophic peatland: implications for modeling and upscaling, Soil Biology and Biochemistry, 41, 1315-1323, 2009b.

Drewer, J., Lohila, A., Aurela, M., Laurila, T., Minkkinen, K., Penttila, T., Dinsmore, K. J., McKenzie, R. M., Helfter, C., Flechard, C., Sutton, M. A., and Skiba, U. M.: Comparison of greenhouse gas fluxes and nitrogen budgets from an ombotrophic bog in Scotland and a minerotrophic sedge fen in Finland, European Journal of Soil Science, 61, 640-650, 2010a.

20 Drewer, J., Lohila, A., Aurela, M., Laurila, T., Minkkinen, K., Penttilä, T., Dinsmore, K. J., McKenzie, R. M., Helfter, C., Flechard, C., Sutton, M. A., and Skiba, U. M.: Comparison of greenhouse gas fluxes and nitrogen budgets from an ombotrophic bog in Scotland and a minerotrophic sedge fen in Finland, European Journal of Soil Science, 61, 640-650, 2010b.

Firestone, M. K. and Davidson, E. A.: Microbiological basis of NO and N_2O productionand consumption in soil In: Exchange of Trace Gases between Terrestrial Ecosystems and the Atmosphere, Andreae, M. O. and Schimel, D. S. (Eds.), John Wiley
25 & Sons, Chichester, 1989.

Freeman, C., Hudson, J., Lock, M. A., Reynolds, B., and Swanson, C.: A possible role of sulphate in the suppresion of wetland methane fluxes following drought, Soil Biology and Biochemistry, 26, 1439-1442, 1994.

Gorham, E.: Northern peatlands - role in the carbon cycle and probable responses to climatic warming, Ecological Applications, 1, 182-195, 1991.

30 Gray, A., Levy, P. E., Cooper, M. D. A., Jones, T., Gaiawyn, J., Leeson, S. R., Ward, S. E., Dinsmore, K. J., Drewer, J., Sheppard, L. J., Ostle, N. J., Evans, C. D., Burden, A., and Zieliński, P.: Methane indicator values for peatlands: a comparison of species and functional groups, Global Change Biology, 19, 1141-1150, 2013.

Hargreaves, K. J. and Fowler, D.: Quantifying the effects of water table and soil temperature on the emission of methane from peat wetland at the field scale, Atmospheric Environment, 32, 3275-3282, 1998.

Hartley, I. P., Hill, T. C., Wade, T. J., Clement, R. J., Moncrieff, J. B., Prieto-Blanco, A., Disney, M. I., Huntley, B., Williams, M., Howden, N. J. K., Wookey, P. A., and Baxter, R.: Quantifying landscape-level methane fluxes in subarctic Finland using a multiscale approach, Global Change Biology, 21, 3712-3725, 2015.

Huttunen, J. T., Nykanen, H., Turunen, J., and Martikainen, P. J.: Methane emissions from natural peatlands in the northern boreal zone in Finland, Fennoscandia. In: Atmospheric Environment, Pergamon Press, Oxford, 2003.

Kettunen, A., Kaitala, V., Lehtinen, A., Lohila, A., Alm, J., Silvola, J., and Martikainen, P. J.: Methane production and oxidation potentials in relation to water table fluctuations in two boreal mires, Soil Biology and Biochemistry, 31, 1741-1749, 1999.

Koven, C. D., Ringeval, B., Friedlingstein, P., Ciais, P., Cadule, P., Khvorostyanov, D., Krinner, G., and Tarnocai, C.: Permafrost carbon-climate feedbacks accelerate global warming, Proceedings of the National Academy of Sciences of the United States of America, 108, 14769-14774, 2011.

Levy, P. E., Burden, A., Cooper, M. D. A., Dinsmore, K. J., Drewer, J., Evans, C., Fowler, D., Gaiawyn, J., Gray, A., Jones, S. K., Jones, T., McNamara, N. P., Mills, R., Ostle, N., Sheppard, L. J., Skiba, U., Sowerby, A., Ward, S. E., and Zieli?ski, P.: Methane emissions from soils: synthesis and analysis of a large UK data set, Global Change Biology, 18, 1657-1669, 2012.

Levy, P. E., Gray, A., Leeson, S. R., Gaiawyn, J., Kelly, M. P. C., Cooper, M. D. A., Dinsmore, K. J., Jones, S. K., and Sheppard, L. J.: Quantification of uncertainty in trace gas fluxes measured by the static chamber method, European Journal of Soil Science, 62, 811-821, 2011.

MacDonald, J. A., Fowler, D., Hargreaves, K. J., Skiba, U., Leith, I. D., and Murray, M. B.: Methane emission rates from a northern wetland; response to temperature, water table and transport, Atmospheric Environment, 32, 3219-3227, 1998.

MacIntyre, S., Wanninkhof, R., and Chanton, J.: Trace gas Exchange across the air-water interface in freshwater and coastal marine environments. In: Biogenic Trace Gases: Measuring emissions from soil and water, Matson, P. A. and Harriss, R. C. (Eds.), Blackwell Science Inc., Cambridge, MA, 1995.

Minkkinen, K. and Laine, J.: Vegetation heterogeneity and ditches create spatial variability in methane fluxes from peatlands drained for forestry, Plant and Soil, 285, 289-304, 2006.

Moosavi, S. C. and Crill, P. M.: Controls on CH_4 and CO_2 emissions along two moisture gradients in the Canadian boreal zone, Journal of Geophysical Research: Atmospheres, 102, 29261-29277, 1997.

Nykanen, H., Alm, J., Silvola, J., Tolonen, K., and Martikainen, P. J.: Methane fluxes on boreal peatlands of different fertility and the effect of long-term experimental lowering of the water table on flux rates, Global Biogeochemical Cycles, 12, 53-69, 1998.

Olefeldt, D., Turetsky, M. R., Crill, P. M., and McGuire, A. D.: Environmental and physical controls on northern terrestrial methane emissions across permafrost zones, Global Change Biology, 19, 589-603, 2013.

O'Shea, S. J., Allen, G., Gallagher, M. W., Bower, K., Illingworth, S. M., Muller, J. B. A., Jones, B., Percival, C. J., Bauguitte, S. J. B., Cain, M., Warwick, N., Quiquet, A., Skiba, U., Drewer, J., Dinsmore, K., Nisbet, E. G., Lowry, D., Fisher, R. E., France, J. L., Aurela, M., Lohila, A., Hayman, G., George, C., Clark, D., Manning, A. J., Friend, A. D., and Pyle, J.: Methane

and carbon dioxide fluxes and their regional scalability for the European Arctic wetlands during the MAMM project in summer 2012, Atmos. Chem. Phys. Discuss., 14, 8455-8494, 2014.

Pachauri, R. K. and Reisinger, A.: Observed effects of climate change. In: Intergovernmental Panel on Climate Change. Climate Change 2007: Synthesis report., Geneva, 2007.

Pelletier, L., Moore, T. R., Roulet, N. T., Garneau, M., and Beaulieu-Audy, V.: Methane fluxes from three peatlands in the La Grande Riviere watershed, James Bay lowland, Canada, J. Geophys. Res.-Biogeosci., 112, 2007.

Pihlatie, M., Pumpanen, J., Rinne, J., Ilvesniemi, H., Simojoki, A., Hari, P., and Vesala, T.: Gas concentration driven fluxes of nitrous oxide and carbon dioxide in boreal forest soil, Tellus B, 59, 458-469, 2007.

Segers, R.: Methane production and methane consumption: a review of processes underlying wetland methane fluxes, Biogeochemistry, 41, 23-51, 1998.

Strack, M., Waddington, J. M., and Tuittila, E. S.: Effect of water table drawdown on northern peatland methane dynamics: implications for climate change. In: Global Biogeochemical Cycles, American Geophysical Union, Washington, 2004.

Sutton, M. A., ., eds. and et al.: The European Nitrogen Assessment, Cambridge University Press, 2011.

Tuomenvirta, H., Drebs, A., Førland, E., Tveito, O.-E., Alexandersson, H., Vaarby Laursen, E., and Jónsson, T.: Nordklim data set 1.0 - Description and illustrations, Norwegian Meteorological Institute, Oslo, 27 pp., 2001.

Tupek, B., Minkkinen, K., Pumpanen, J., Vesala, T., and Nikinmaa, E.: CH_4 and N_2O dynamics in the boreal forest–mire ecotone, Biogeosciences Discuss., 11, 8049-8084, 2014.

Turetsky, M. R., Kotowska, A., Bubier, J., Dise, N. B., Crill, P., Hornibrook, E. R. C., Minkkinen, K., Moore, T. R., Myers-Smith, I. H., Nykänen, H., Olefeldt, D., Rinne, J., Saarnio, S., Shurpali, N., Tuittila, E.-S., Waddington, J. M., White, J. R., Wickland, K. P., and Wilmking, M.: A synthesis of methane emissions from 71 northern, temperate, and subtropical wetlands, Global Change Biology, 20, 2183-2197, 2014.

Waddington, J. M., Roulet, N. T., and Swanson, R. V.: Water table control of CH_4 emission enhancement by vascular plants in boreal peatlands, Journal of Geophysical Research-Atmospheres, 101, 22775-22785, 1996.

Yvon-Durocher, G., Allen, A. P., Bastviken, D., Conrad, R., Gudasz, C., St-Pierre, A., Thanh-Duc, N., and del Giorgio, P. A.: Methane fluxes show consistent temperature dependence across microbial to ecosystem scales, Nature, 507, 488-491, 2014.

Zhu, X., Zhuang, Q., Qin, Z., Glagolev, M., and Song, L.: Estimating wetland methane emissions from the northern high latitudes from 1990 to 2009 using artificial neural networks, Global Biogeochemical Cycles, 27, 592-604, 2013.

Tables

Table 1. Mean ± SE CH_4 and N_2O fluxes split by both campaign period (summer, autumn) and site (forest, wetland).

	Summer	Autumn	Full Period
CH_4 (mg C m^{-2} hr^{-1})			
Forest	-0.06 ± <0.01	-0.03 ± <0.01	-0.04 ± <0.01
Wetland	3.35 ± 0.44	0.62 ± 0.09	1.56 ± 0.20
N_2O (μg N m^{-2} hr^{-1})			
Forest	0.75 ± 0.33	1.29 ± 1.39	1.06 ± 0.44
Wetland	1.63 ± 0.64	-1.60 ± 1.18	0.73 ± 0.40

5   Table 2. Mean ± stdev ground cover data for wetland clusters. Only variables which showed significant between cluster variability are included. Test statistic refers to the F-value with * and ** indicating P-vales of <0.05 and <0.01, respectively.

	Sphagnum sp.	Openwater
Wetland_a	39.3 ± 46.0	59.5 ± 62.0
Wetland_b	68.6 ± 47.4	11.4 ± 18.6
Wetland_c	95.7 ± 11.3	5.71 ± 9.32
Wetland_d	50.0 ± 70.7	20.0 ± 28.2
ANOVA test statistic	4.62**	3.59*

Table 3. Model summary utilising spectral data to estimate CH_4 emissions

	Estimate	t-value	p-value
Intercept	-233	0.00002	<0.01
SR	354	0.00002	<0.01
NDVI	-283	0.03883	<0.05
Blue	0.99	0.00365	<0.01
NIR	-0.91	0.00022	<0.01
model r^2	0.45		
model p-value	<0.01		

Figures
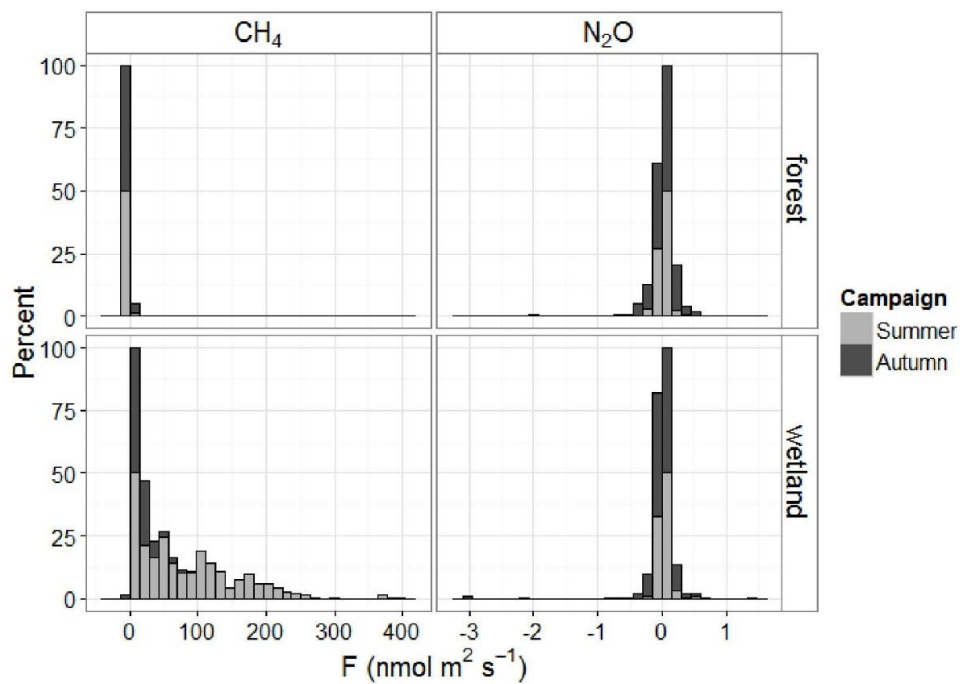
Figure 1. Frequency plot showing distribution of all fluxes across both campaign periods
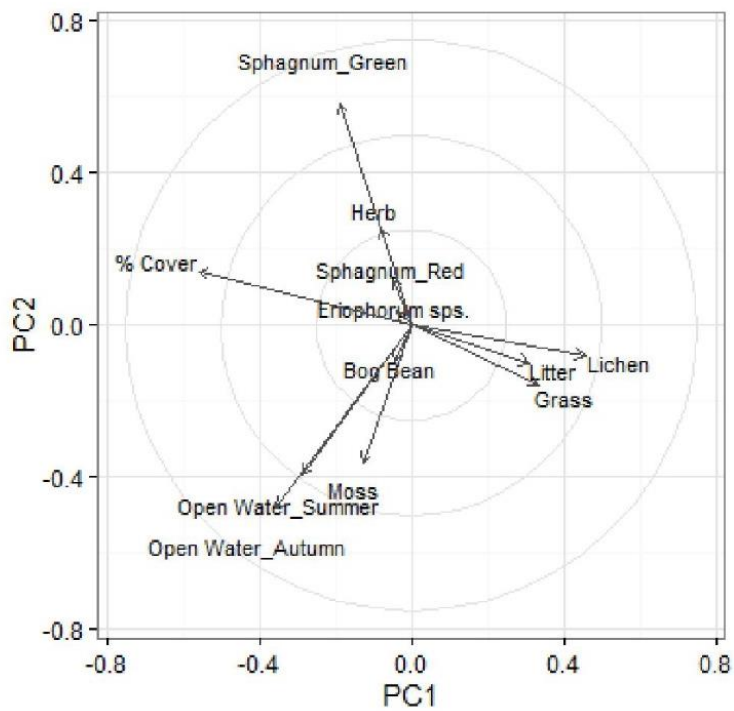
Figure 2. Loading values for principal components 1 and 2 of the chamber vegetation analysis
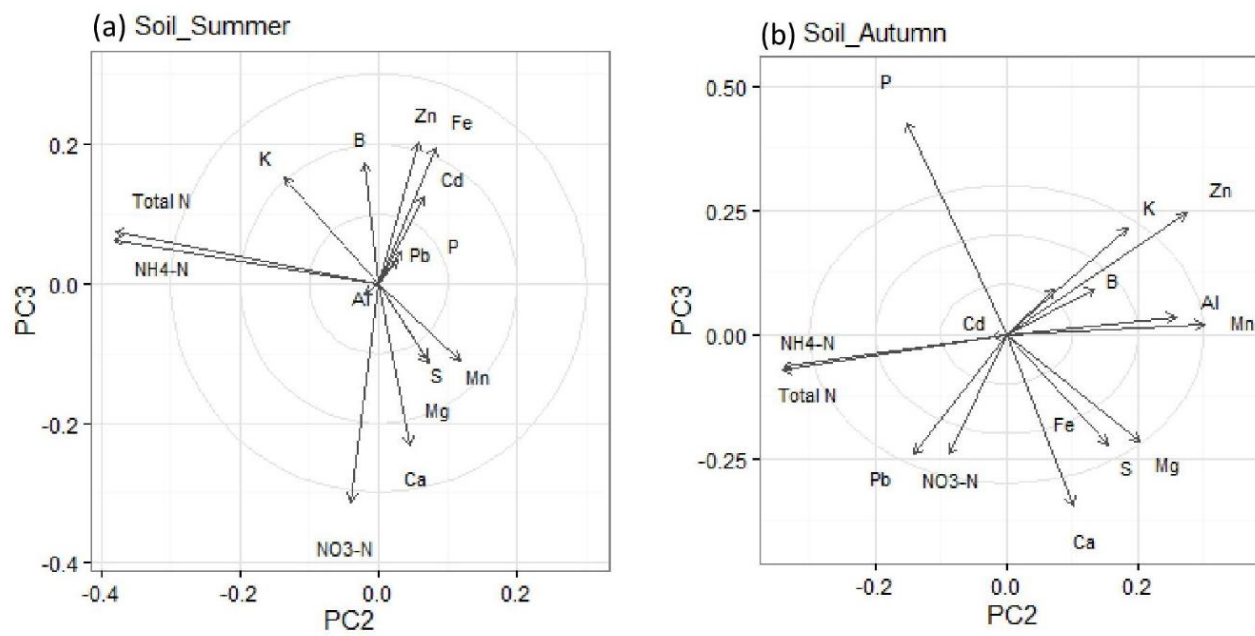
Figure 3. Loading values for principal components 1 and 2 of the chamber soil concentration analysis
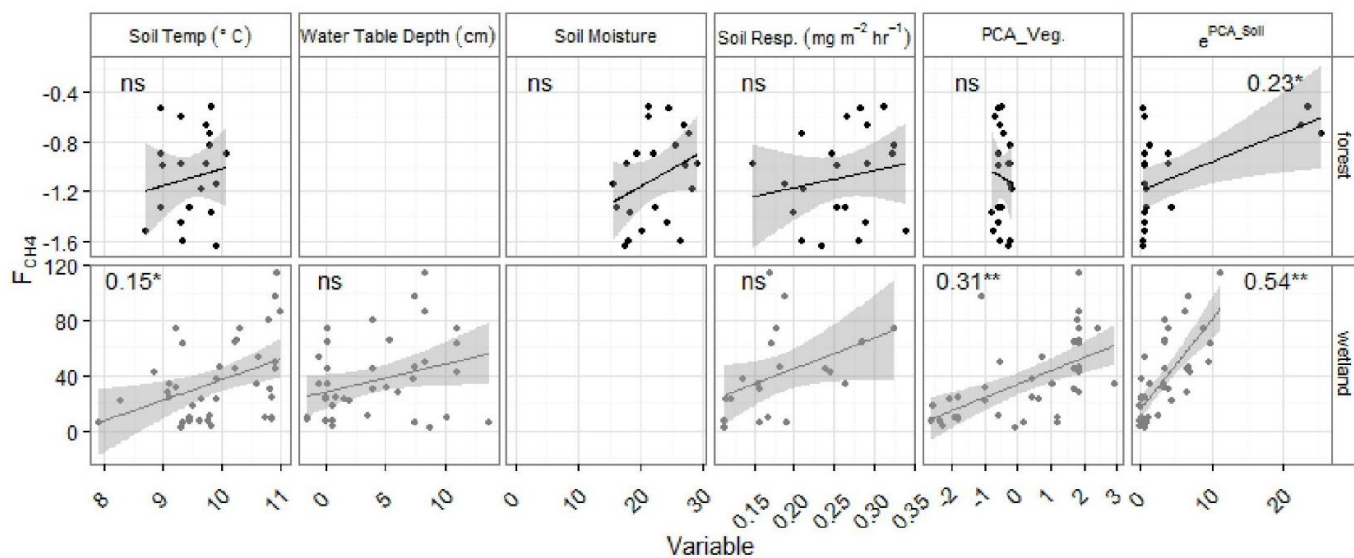
5   Figure 4. Relationships between geometric mean CH$_4$ flux (nmol m^{-2} s^{-1}) against measured environmental variables. Text refers to the results from statistical correlations were 'ns' refers to a non-significant results, * and ** represent $P < 0.05$ and $P < 0.01$, respectively.
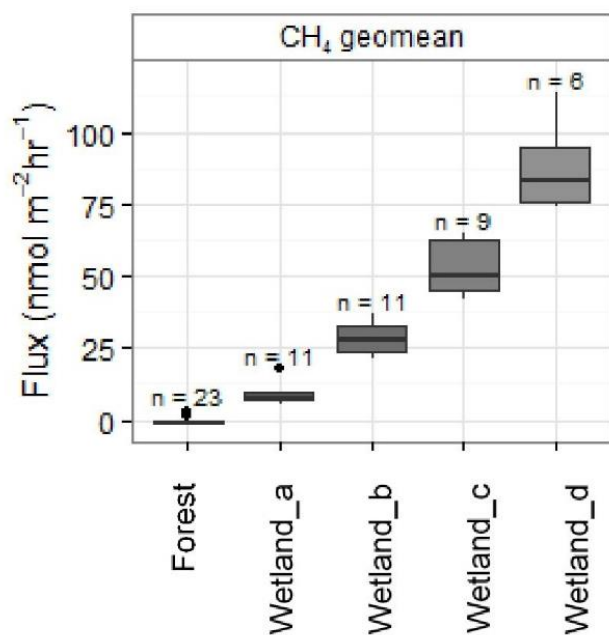
Figure 5. Chambers clustered based on emissions with n indicating the number of chambers within each group.
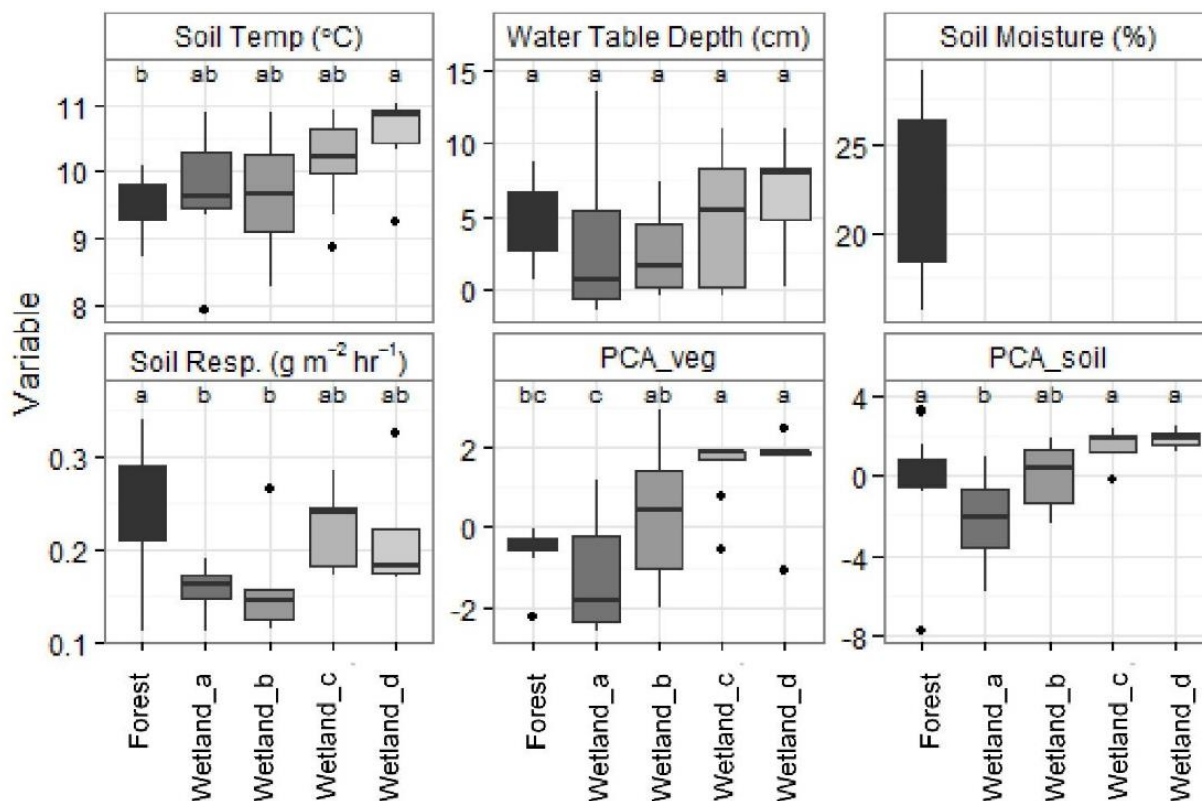
Figure 6. Boxplots showing range of measured environmental variables within each of the CH_4 clusters. Letters represent results from Tukeys family test statistic where clusters with similar letters are not significantly different from one another at 95% confidence level. Clusters Wetland_a to Wetland_d represent groups with sequentially increasing CH_4 emissions.
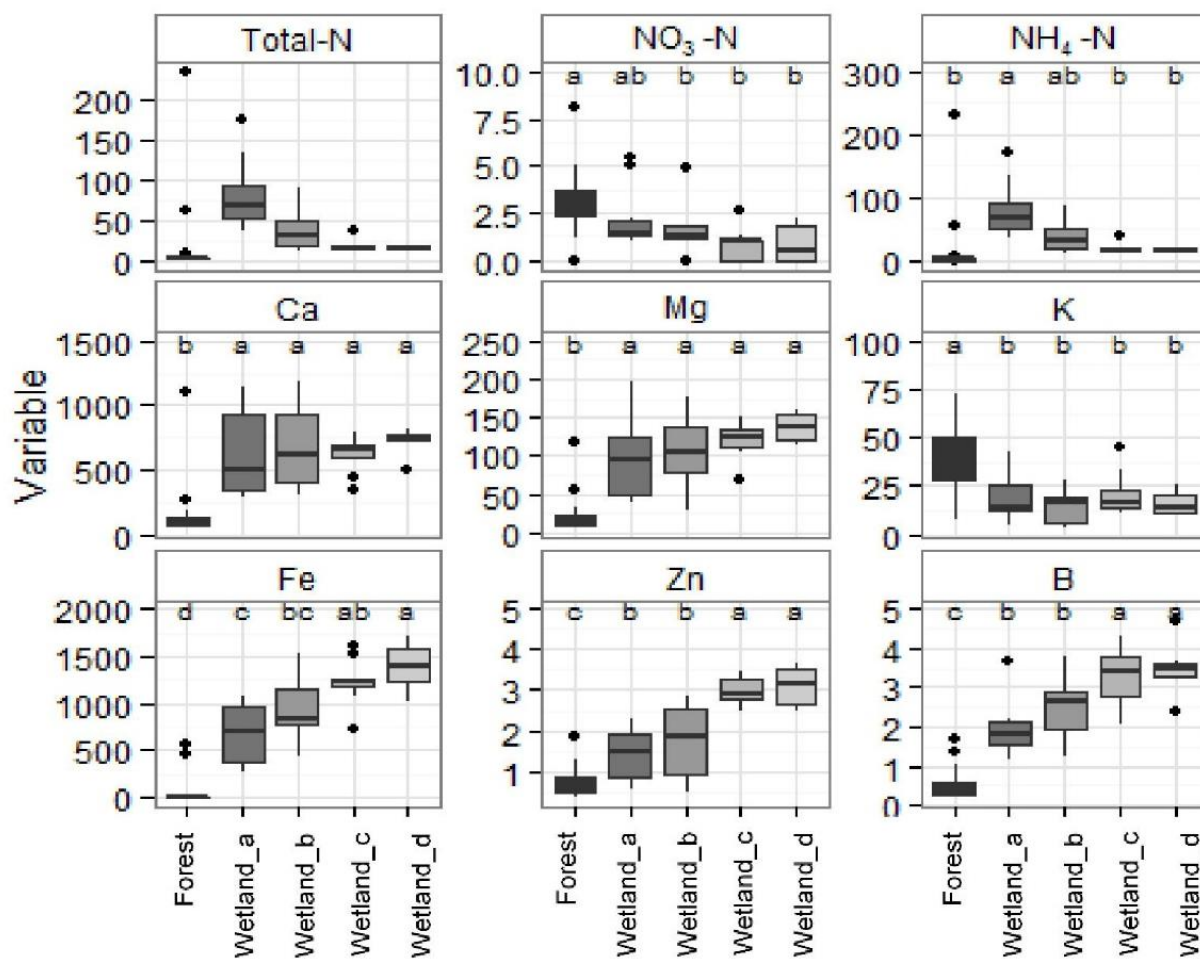
Figure 7. Boxplots showing range of soil variables within each of the CH$_4$ clusters. Letters represent results from Tukeys

family test statistic where clusters with similar letters are not significantly different from one another at 95% confidence level.

Clusters Wetland_a to Wetland_d represent groups with sequentially increasing CH$_4$ emissions.
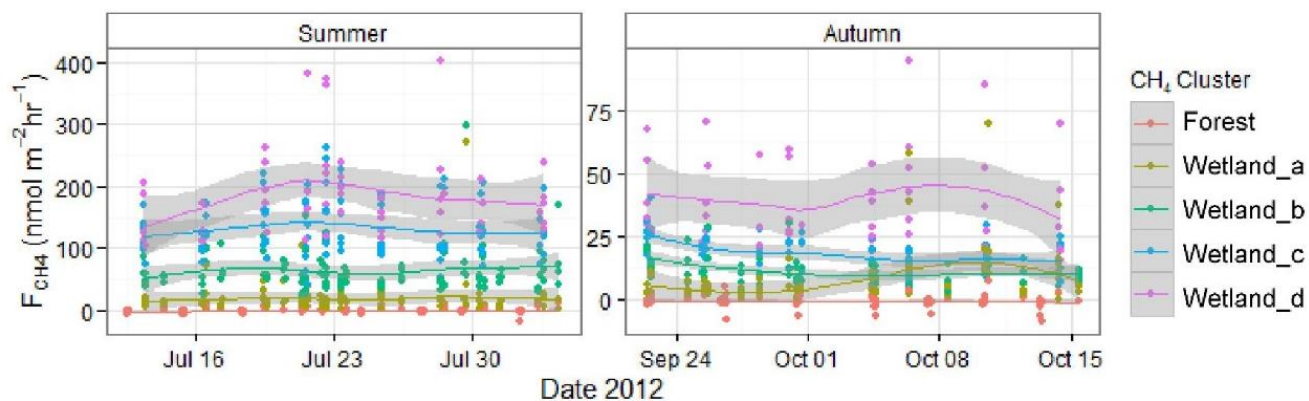
5   Figure 8. Temporal variability across the 2 field campaigns in CH$_4$ emissions, separated by clusters, with shaded area representing loess smoothing. Clusters Wetland_a to Wetland_d represent groups with sequentially increasing CH$_4$ emissions.
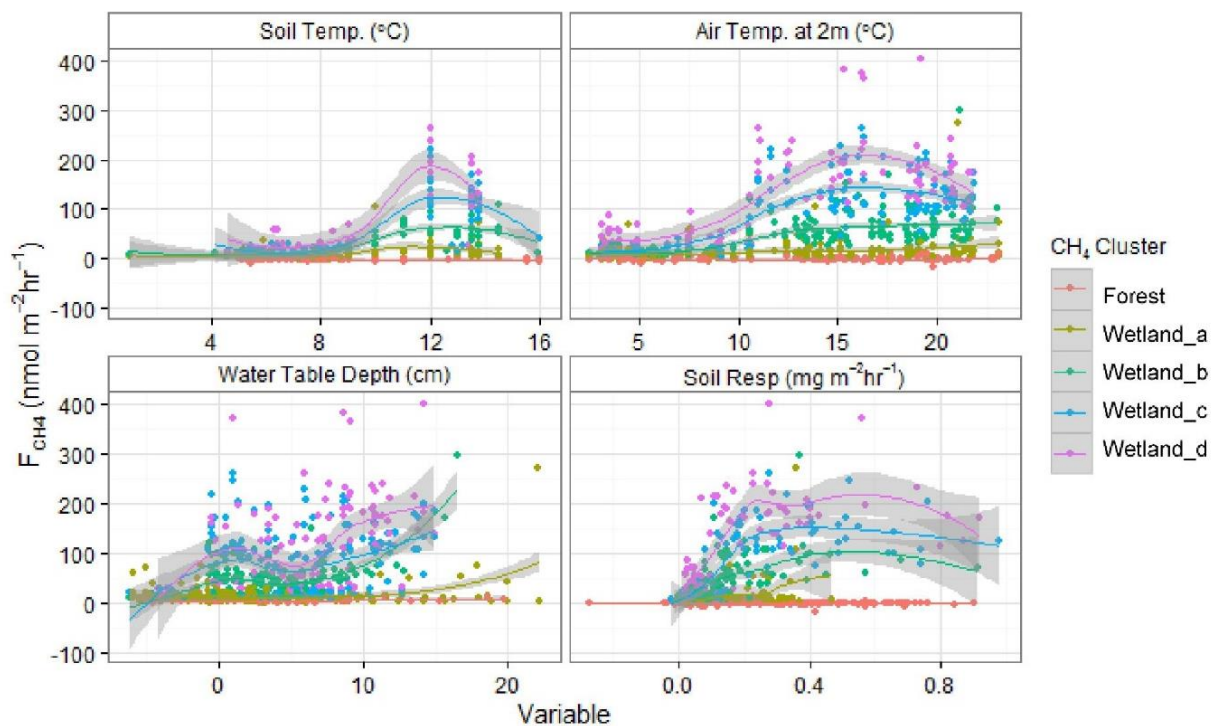
Figure 9. Drivers of temporal variability in CH₄ fluxes, separated by clusters, with shaded area representing loess smoothing. Clusters Wetland_a to Wetland_d represent groups with sequentially increasing CH₄ emissions.
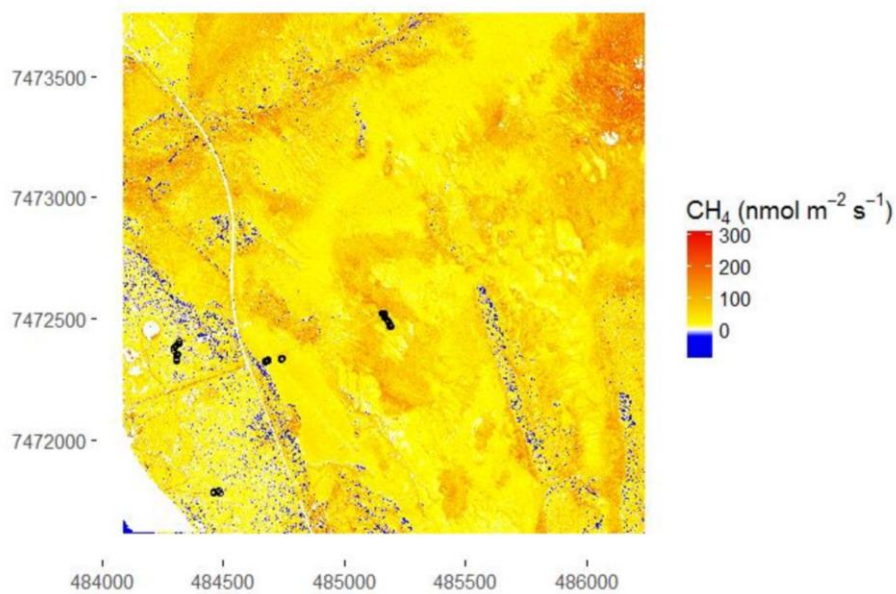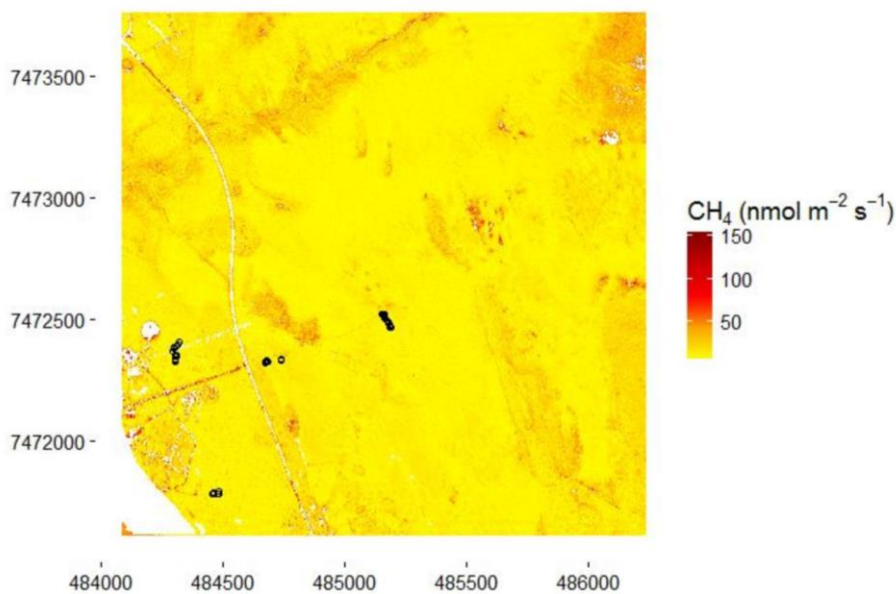
Figure 10. Mean (a) and SE (b) of CH$_4$ fluxes extrapolated over a 2 x 2 km area predicted from chamber flux measurements (black circles), and satellite spectral data. Coordinates are in WGS84.